Journal of Coordination Chemistry

ISSN: 0095-8972 (Print) 1029-0389 (Online) Journal homepage: http://www.tandfonline.com/loi/gcoo20

Zeolite-Y encapsulated nanohybrid materials: synthesis, spectroscopic characterization, and catalytic significance

C.K. Modi & Parthiv M. Trivedi

To cite this article: C.K. Modi & Parthiv M. Trivedi (2012) Zeolite-Y encapsulated nanohybrid materials: synthesis, spectroscopic characterization, and catalytic significance, Journal of Coordination Chemistry, 65:3, 525-538, DOI: 10.1080/00958972.2012.656616

To link to this article: http://dx.doi.org/10.1080/00958972.2012.656616

Published online: 02 Feb 2012.

Journal of Coordination Chemistry
Vol. 65, No. 3, 10 February 2012, 525–538

Taylor & Francis
Taylor & Francis Group

Zeolite-Y encapsulated nanohybrid materials: synthesis, spectroscopic characterization, and catalytic significance

C.K. MODI* and PARTHIV M. TRIVEDI

Department of Chemistry, Bhavnagar University, Bhavnagar – 364 002, Gujarat, India

(*Received 19 September 2011; in final form 12 December 2011*)

The goal of this study is to synthesize zeolite-Y encapsulated nanohybrid materials (ZENMs) of the general formulae $[M(VTCH)_2]$-Y or $[M(VFCH)_2]$-Y (where M = Mn(II), Co(II), Ni(II), and Cu(II); VTCH = vanillin thiophene-2-carboxylic hydrazone; VFCH = vanillin furoic-2-carboxylic hydrazone) and describe their selective catalytic activities. ZENMs are characterized by various physico-chemical techniques, namely ICP-OES, elemental analysis, (FT-IR and electronic) spectral studies, SEMs, X-ray diffraction patterns as well as surface area measurements. The catalytic activities of ZENMs were found to be highly advantageous in yielding significant amounts of cyclohexanone and cyclohexanol in the liquid-phase oxidation of cyclohexane.

Keywords: Zeolite-Y; Encapsulated nanohybrid materials; Oxidation of cyclohexane

1. Introduction

Oxidation of cyclohexane is an industrial process of great importance but to date of little efficiency [1–4]. The classic homogeneous process of cyclohexane oxidation to give cyclohexanone and cyclohexanol is carried out with air using cobalt catalysts at 443–503 K and high pressures (10–15 bar) [5]. In this homogeneous process, cyclohexane conversion is lower than 10% (usually around 4%) and very low yields of cyclohexanol and cyclohexanone are obtained [6]. As a consequence, oxidation of cyclohexane continues to be a challenge [7] and attention has been devoted to heterogenizing homogeneous catalysts onto solid supports to increase catalyst stability and allow for catalyst recycling and product separation [8–13]. Generally, homogeneous catalysts are heterogenized either through covalent attachment or encapsulation into porous supports, like MCM-41 [14], SBA-15 [15], and zeolite-Y [16–18].

Zeolite crystals are porous on a molecular scale, with internal pores containing regular arrays of channels and cavities with regular dimensions, but of different sizes and shapes. In particular, the structure of zeolite-Y consists of almost spherical 1.3 nm (13 Å) cavities interconnected tetrahedrally through smaller apertures of 0.74 nm (7.4 Å) diameters [19, 20]. The exchangeable properties of extra-framework cations and the suitable cavity size of the zeolites allow their modification by inclusion of homogeneous

*Corresponding author. Email: chetank.modi1@gmail.com

Journal of Coordination Chemistry
ISSN 0095-8972 print/ISSN 1029-0389 online
http://dx.doi.org/10.1080/00958972.2012.656616

catalysts (i.e. metal complexes with regular Oh, Td, square planar, square pyramidal, or distorted geometries). The use of transition metal complexes encapsulated into zeolitic framework as heterogeneous catalysts has become very important for eco-friendly industrial processes [21]. The encapsulation strategy is convenient and advantageous because the metal complex once formed inside the pore cavity does not easily diffuse out into the liquid phase during catalytic reaction.

Zeolite-Y encapsulated nanohybrid materials (ZENMs) are crystalline materials assembled by bonding of metal ions with Schiff-base ligands. ZENMs with nano-sized channels offer great potential for direct incorporation of catalytic sites. It could be expected that ZENMs containing uniformly sized and shaped pores could open possibilities for size- and shape-selectivity effects. Their attributes include high porosity, spatial and chemical tailoring, and synthetic scalability [22, 23]. They have attracted great attention due to their various potential applications in catalysis, adsorption, separation, etc. [24–40].

In continuous search for new processes for oxidation of cyclohexane [41, 42], herein we report synthesis, spectroscopic, and catalytic significance of ZENMs. The potential benefits of this study are threefold: (1) to produce novel ZENMs by encapsulation of transition metal complexes of Schiff bases (figure 1) vanillin thiophene-2-carboxylic hydrazone (VTCH) and vanillin furoic-2-carboxylic hydrazone (VFCH) in the nanovoids of zeolite-Y by flexible ligand method (FLM), (2) to characterize ZENMs by various physico-chemical techniques, and (3) to screen ZENMs for their catalytic activity over liquid-phase oxidation of cyclohexane.

2. Experimental

2.1. *Materials and physical measurements*

All chemicals and solvents were of AR grade and used without purification. Thiophene-2-carboxylic acid, furoic-2-carboxylic acid, and vanillin were obtained from Spectrochem (India) and 30% H_2O_2 was purchased from Rankem (India). Sodium form of zeolite-Y (Si/Al = 2.60) was procured from Hi-media, India. Carbon, hydrogen, and nitrogen were analyzed with a Perkin Elmer, USA 2400-II CHN analyzer. Si, Al,

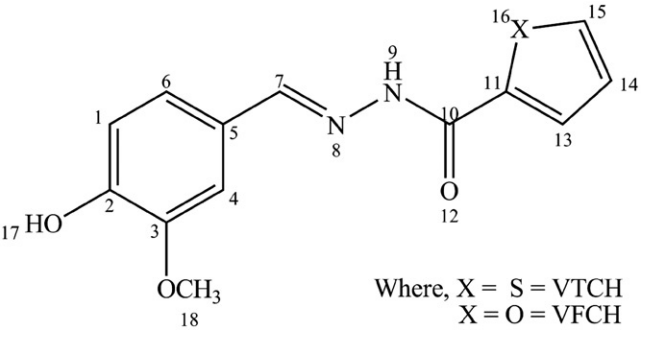

Figure 1. Schiff-base ligands (VTCH and VFCH) under study.

Na, and transition metal ions in the encapsulated nanohybrid materials were determined by ICP-OES (Model: Perkin Elmer optima 2000 DV). Infrared (IR) spectra of encapsulated hybrid materials were recorded on a Thermo Nicolet IR 200 FT-IR spectrometer. The crystallinity was ensured by X-ray diffraction (XRD) using a Bruker AXS D_8 Advance X-ray powder diffractometer with a Cu-Kα target. The surface area of encapsulated nanohybrid materials was measured by multipoint BET method using a Micromeritics, ASAP 2010 surface area analyzer. The gas chromatography–mass spectrometry (GC-MS) of Schiff-base ligands were recorded on a Shimadzu, QP-2010 equipped with a RTX-5 column. The scanning electron micrographs (SEMs) of encapsulated nanohybrid materials were recorded using an SEM instrument (Model: LEO 1430 VP). ^{1}H- and ^{13}C-NMR spectra of Schiff-base ligands were recorded on a Avance 400 Bruker FT-NMR instrument with DMSO-d_6 as solvent.

2.2. *Synthesis of VTCH*

An ethanolic solution (25 mL) of thiophene-2-carboxylic hydrazide (10 mmol, 1.42 g) and an ethanolic solution (25 mL) of vanillin (10 mmol, 1.52 g) in 1 : 1 molar ratio were mixed with constant stirring and refluxed for 4 h. The solution was cooled overnight at room temperature. Light yellow crystals of VTCH were collected and dried in air. Yield, 72%; m.p. 206°C. Found (%): C, 56.16; H, 4.15; N, 9.58; O, 17.06; S, 11.34. $C_{13}H_{12}N_2O_3S$ requires (%): C, 56.51; H, 4.38; N, 10.14; O, 17.37; S, 11.60. ^{1}H-NMR (400 MHz, DMSO-d_6): δ 3.83 (3H, s, –CH_3), 7.05–7.28 (3H, m, Ar–H), 7.30–8.28 (3H, m, thiophene ring-H), 8.3 (1H, s, –CH=N), 9.6 (1H, s, –NH), 11.7 (1H, s, –OH). *m*/*z*: 277.17, 193.08, 166, 149.92, 127, 111.10, 94. ^{13}C-NMR (400 MHz, DMSO-d_6): δ (ppm) = 56.0 (C_{19}), 114.7 (C_4), 116.2 (C_1), 119.1 (C_6), 124.0 (C_{14}), 128.7 (C_{15}), 129.8 (C_{13}), 131.3 (C_5), 137.1 (C_{11}), 145.8 (C_7), 149.1 (C_3), 149.9 (C_2), 168.6 (C_{10}).

2.3. *Synthesis of VFCH*

The Schiff base (VFCH) was prepared the same way as VTCH. Yield, 68%; m.p. 210°C. Found (%): C, 59.37; H, 4.32; N, 9.69; O, 24.26. $C_{13}H_{12}N_2O_4$ requires (%): C, 60.00; H, 4.65; N, 10.76; O, 24.59. ^{1}H-NMR (400 MHz, DMSO-d_6): δ 3.83 (3H, s, –CH_3), 7.07–7.28 (3H, m, Ar–H), 6.84–7.29 (3H, m, furoic ring-H), 8.4 (1H, s, –CH=N), 9.5 (1H, s, –NH), 11.6 (1H, s, –OH). *m*/*z*: 260, 150, 134, 111, 95, 77, 67. ^{13}C-NMR (400 MHz, DMSO-d_6): δ (ppm) = 56.0 (C_{19}), 109.4 (C_4), 112.4 (C_{14}), 115.0 (C_{13}), 115.9 (C_1), 122.7 (C_6), 126.1 (C_5), 146.1 (C_{15}), 147.3 (C_7), 148.5 (C_{11}), 149.0 (C_3), 149.5 (C_2), 154.5 (C_{10}).

2.4. *Synthesis of M^{II}-Y (metal-exchanged zeolite-Y)*

Na-Y zeolite (5.0 g) was suspended in 300 mL of deionized water containing 12 mmol metal salts [$Mn(CH_3COO)_2 \cdot 4H_2O$, $Co(CH_3COO)_2 \cdot 4H_2O$, $Ni(CH_3COO)_2 \cdot 4H_2O$, and $Cu(CH_3COO)_2 \cdot H_2O$] with constant stirring. The reaction mixture was then heated at 90°C for 24 h. The solid was filtered, washed with hot deionized water until the filtrate was free from any metal ion content, and dried for 15 h at 150°C in air.

2.5. *Synthesis of [M(VTCH)$_2$]-Y and [M(VFCH)$_2$]-Y*

ZENMs were prepared using the FLM. First, 1.0 g of M^{II}-Y was thoroughly mixed with an excess of VTCH ($n_{ligand}/n_{metal} = 3$) in ethanol and sealed into a round bottom flask. The reaction mixture was refluxed (~24 h) in an oil bath with stirring under inert atmosphere. The resulting material was taken out, followed by Soxhlet extraction with ethanol, acetone and finally with acetonitrile (6 h) to remove uncomplexed ligand and the complex adsorbed on the exterior surface of zeolite-Y. The extracted sample was ion-exchanged with 0.01 mol L^{-1} NaCl aqueous solution for 24 h to remove uncoordinated M^{II} ions, followed by washing with deionized water until no Cl^- could be detected with $AgNO_3$ solution. The product was collected and dried at 120°C. The same procedure was applied for the preparation of [M(VFCH)$_2$]-Y.

2.6. *Catalytic experiments*

Catalytic activity of ZENMs was evaluated for liquid-phase oxidation of cyclohexane with 30% H_2O_2 as an oxidizing agent. Reaction conditions for the liquid-phase oxidation of cyclohexane were optimized as follows: cyclohexane (10 mmol), 30% H_2O_2 (10 mmol), catalyst (60 mg), acetonitrile (2 mL) at 80°C for 2 h. ZENMs catalyzed oxidation of cyclohexane gives cyclohexanol (CyOL) and cyclohexanone (CyONE). The progress of the reaction was monitored as a function of time by withdrawing portions of the sample at 30 min. time intervals and analyzing them by GC.

3. Results and discussion

3.1. *Morphological and textural properties of materials*

Chemical analyses of the neat zeolite-Y and ZENMs reveal the presence of organic matter with a C/N ratio as given in table 1. Moreover, the Si/Al ratio is 2.60 for the neat zeolite-Y, indicating no dealumination during the encapsulation by FLM. The surface area and pore volume values estimated by nitrogen adsorption isotherms are given in table 2. The results exhibit a decrease in surface area and pore volume of zeolite-Y on encapsulation of metal complexes, which show the presence of complexes inside the nanovoids of zeolite-Y [43, 44].

Figure 2 presents SEMs of [Ni(VTCH)$_2$]-Y recorded before and after Soxhlet extraction. It is clear from the well-defined crystals after Soxhlet extraction that ZENMs have no surface complexes and the particle boundaries on the external surface of zeolite-Y are clearly distinguishable. These micrographs reveal the efficiency of the purification procedure to effect removal of extraneous complexes, leading to the presence of well-defined encapsulation in the cavity.

The powder XRD patterns of Na-Y and ZENMs are presented in figure 3. Similar diffraction patterns were observed for ZENMs, except small change in relative peak intensities. This indicates that the crystallinity of the zeolitic matrix remained intact with no major structural modifications upon encapsulation of the metal complex. This is further supported by SEMs analysis that all ZENMs retain the crystallinity of the zeolite-Y.

Table 1. Analytical and physical data of compounds.

Sr. no.	Compounds	Elements % found								
		%C	%H	%N	C/N	%Si	%Al	%Na	%M	Si/Al
1	Na-Y	–	–	–	–	17.16	6.60	9.86	–	2.60
2	Mn^{II}-Y	–	–	–	–	17.08	6.56	5.68	2.40	2.60
3	$[Mn(VTCH)_2]$-Y	4.72	1.41	0.95	4.97	16.61	6.39	7.30	2.19	2.60
4	$[Mn(VFCH)_2]$-Y	4.76	1.45	0.96	4.95	16.73	6.43	6.81	2.20	2.60
5	Co^{II}-Y	–	–	–	–	16.80	6.46	4.87	3.53	2.60
6	$[Co(VTCH)_2]$-Y	4.85	1.48	1.03	4.61	16.55	6.36	5.88	2.22	2.60
7	$[Co(VFCH)_2]$-Y	4.88	1.52	1.06	4.60	16.49	6.34	6.05	2.24	2.60
8	Ni^{II}-Y	–	–	–	–	16.98	6.53	3.92	3.62	2.60
9	$[Ni(VTCH)_2]$-Y	4.80	1.47	1.06	4.52	16.40	6.30	5.42	2.28	2.60
10	$[Ni(VFCH)_2]$-Y	4.78	1.50	1.04	4.56	16.45	6.32	5.52	2.27	2.60
11	Cu^{II}-Y	–	–	–	–	16.90	6.50	7.01	4.71	2.60
12	$[Cu(VTCH)_2]$-Y	4.69	1.42	0.98	4.78	16.70	6.42	6.20	2.25	2.60
13	$[Cu(VFCH)_2]$-Y	4.65	1.39	0.97	4.75	16.65	6.40	6.33	2.21	2.60

Table 2. Surface area and pore volume data of compounds.

Compounds	Surface area ($m^2\,g^{-1}$)	Pore volume ($cc\,g^{-1}$)[a]
Na-Y	548	0.32
Mn^{II}-Y	538	0.29
$[Mn(VTCH)_2]$-Y	265	0.15
$[Mn(VFCH)_2]$-Y	280	0.19
Co^{II}-Y	530	0.30
$[Co(VTCH)_2]$-Y	272	0.17
$[Co(VFCH)_2]$-Y	276	0.18
Ni^{II}-Y	527	0.30
$[Ni(VTCH)_2]$-Y	269	0.16
$[Ni(VFCH)_2]$-Y	275	0.17
Cu^{II}-Y	534	0.31
$[Cu(VTCH)_2]$-Y	261	0.13
$[Cu(VFCH)_2]$-Y	263	0.14

[a]Calculated by the BJH-method.

3.2. *Spectroscopic characterization*

Table 3 shows a list of FT-IR spectral data of Schiff bases, $[M(VTCH)_2]$-Y and $[M(VFCH)_2]$-Y. The intensity of peaks in ZENMs is weak due to their low concentration in the zeolite matrix. Comparison of the spectra of Schiff bases namely VTCH or VFCH with ZENMs provides evidence for coordinating mode of ligand in ZENMs. The ν(N–H) and ν(C=O) of the lateral chain in the uncoordinated Schiff bases are at 3180–3189 and 1690–1695 cm^{-1}, respectively, indicating that the ligands exist in keto form in the solid state [45]. However, these bands are absent in spectra of ZENMs with a new band at 1344–1353 cm^{-1} due to ν(C–O) [46, 47]. From these observations, the ligand reacts in enol form *via* proton transfer through oxygen forming a bond with the metal ion. The sharp and strong band at 1635–1639 cm^{-1} is due to ν(C=N) of azomethine of the lateral chain. The low-energy shift of this band in spectra of ZENMs,

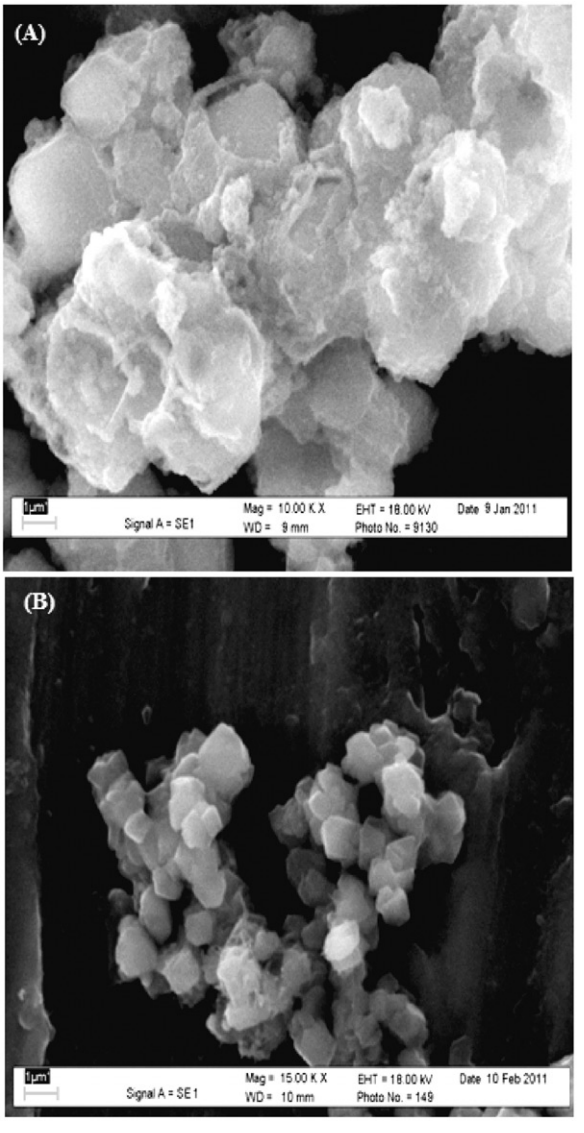

Figure 2. SEM images of $[Ni(VFCH)_2]$-Y (A) before and (B) after Soxhlet extraction.

at ~1620 cm^{-1}, suggests the coordination of azomethine nitrogen [48]. The framework vibration bands of zeolite-Y are below 1200 cm^{-1} for all samples. Bands at 556–583, 720–786, and 1012–1134 cm^{-1} are attributed to double ring, symmetric stretching, and asymmetric stretching vibrations, respectively [49]. No shift is observed upon introduction of metal ions and inclusion of metal complexes, further substantiating that the zeolite-Y framework remains unchanged.

Electronic spectral bands of VTCH and/or VFCH and ZENMs are discussed and tabulated in table 4. From 200 to 800 nm, the electronic spectra of Schiff bases showed an intense band at ~329 nm due to intra-ligand charge transfer transitions ($\pi \rightarrow \pi^*$); this band undergoes bathochromic shifts in Mn(II) and hypsochromic shifts in Co(II)

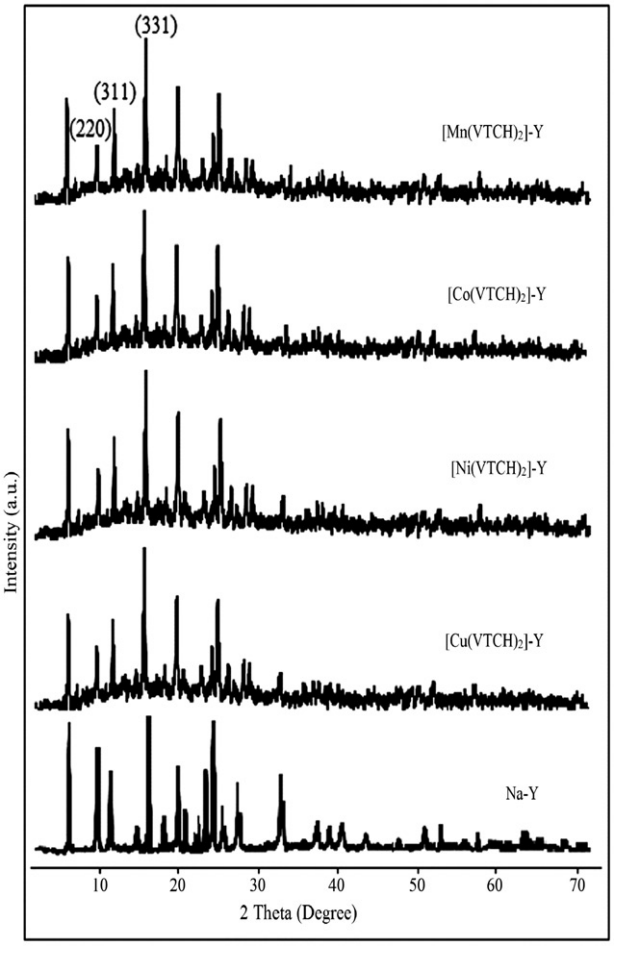

Figure 3. XRD patterns of Na-Y and its modified zeolites.

Table 3. FT-IR assignments of Schiff bases and ZENMs.

	Internal vibrations		External vibrations							
Compounds	ν_{asym}T–O	ν_{sym}T–O	D–R	ν_{sym}T–O	ν_{asym}T–O	$\nu_{(C=N)}$	$\nu_{(C=O)}$	$\nu_{(N-H)}$	$\nu_{(O-H)}$	$\nu_{(C-O)}$
VTCH	–	–	–	–	–	1635	1690	3180	3422	1286
VFCH	–	–	–	–	–	1639	1695	3189	3432	1291
$[Mn(VTCH)_2]$-Y	1017	721	574	786	1120	1616	–	–	3442	1348
$[Mn(VFCH)_2]$-Y	1019	726	569	781	1128	1615	–	–	3448	1344
$[Co(VTCH)_2]$-Y	1027	729	571	769	1134	1624	–	–	3442	1350
$[Co(VFCH)_2]$-Y	1025	728	566	776	1124	1623	–	–	3444	1347
$[Ni(VTCH)_2]$-Y	1012	725	560	770	1120	1618	–	–	3433	1352
$[Ni(VFCH)_2]$-Y	1014	720	556	775	1130	1615	–	–	3438	1345
$[Cu(VTCH)_2]$-Y	1021	730	576	783	1125	1620	–	–	3448	1353
$[Cu(VFCH)_2]$-Y	1025	727	583	780	1122	1622	–	–	3440	1351

Table 4. Electronic spectral data of VTCH, VFCH, and ZENMs.

Compounds	ILCT ($\pi \rightarrow \pi^*$) transition in nm	MLCT transition in nm	d–d transition in nm
VTCH	329	–	–
VFCH	324	–	–
[Mn(VTCH)$_2$]-Y	335	220	–
[Mn(VFCH)$_2$]-Y	333	233	–
[Co(VTCH)$_2$]-Y	323	244	778
[Co(VFCH)$_2$]-Y	322	243	792
[Ni(VTCH)$_2$]-Y	302	–	647
[Ni(VFCH)$_2$]-Y	308	–	630
[Cu(VTCH)$_2$]-Y	–	–	401
[Cu(VFCH)$_2$]-Y	–	–	405

and Ni(II) encapsulated hybrid materials resulting from chelation of the ligand with the transition metal. As expected for Mn(II) encapsulated hybrid materials, d–d transition bands are not observed in dilute solution because of their being doubly forbidden. The spectra of Co(II) encapsulated hybrid materials show two additional absorption bands at ~244 and 792–778 nm attributed to metal-to-ligand charge transfer (MLCT) and $^2B_{2g} \rightarrow {}^2E_g$ transitions, concordant with square-planar structure [50]. The same bands are present in the UV-Vis spectrum of neat Co(VTCH)$_2$ complex, which means the configuration of cobalt complex had no change when encapsulated inside the nanopores of zeolite-Y (figure 4). Square-planar d^8 metal complexes are characterized by three spin allowed d–d bands, $d_{xy}(b_{1g}) \rightarrow d_{x^2-y^2}(b_{1g})$, $d_z^2(a_{1g}) \rightarrow d_{x^2-y^2}(b_{1g})$, and $d_{xz,yz}(e_g) \rightarrow d_{x^2-y^2}(e_g)$ corresponding to $^1A_{1g} \rightarrow {}^1A_{2g}$ (ν_1), $^1A_{1g} \rightarrow {}^1B_{1g}$ (ν_2), and $^1A_{1g} \rightarrow {}^1E_g$ (ν_3) transitions [51]. Of the three expected low energy ligand field (d–d) bands, corresponding to transitions from the three lower d-levels to the empty $d_{x^2-y^2}$ orbitals, only one is observed in the visible spectra of [Ni(VTCH)$_2$]-Y and [Ni(VFCH)$_2$]-Y near 647 nm. This may be assigned to $^1A_{1g} \rightarrow {}^1A_{2g}$ (ν_1) transition of Ni(II) in square-planar structure. The weak band observed near 405 nm for Cu(II) encapsulated hybrid materials is assigned to $^2B_{1g} \rightarrow {}^2E_g$ transition of square-planar geometry [52].

3.3. *Catalytic activity studies*

3.3.1. Oxidation of cyclohexane. Catalytic oxidation of cyclohexane was undertaken in a two-necked 50 mL round bottomed flask. In a typical reaction, 10 mmol of the substrate was taken in 2 mL of acetonitrile, 60 mg of the catalyst added to it and equilibrated at 80°C in an oil bath. 10 mmol of 30% H_2O_2 solution was added to this with continuous stirring for 2 h and the results are given in table 5. Blank experiments performed without catalyst or with Na-Y zeolite show a lesser amount of conversion. The products were collected at different time intervals and identified and quantified by GC. The absence of metal ions in filtrate indicates that no leaching of complexes occurred during reaction, as they are intact in the nanopores [53].

Blank reactions performed over zeolite-Y and M^{II}-Y under identical conditions show only negligible conversion, indicating that zeolite host is inactive for oxidation. The VTCH and VFCH ligands alone in the absence of metal were not

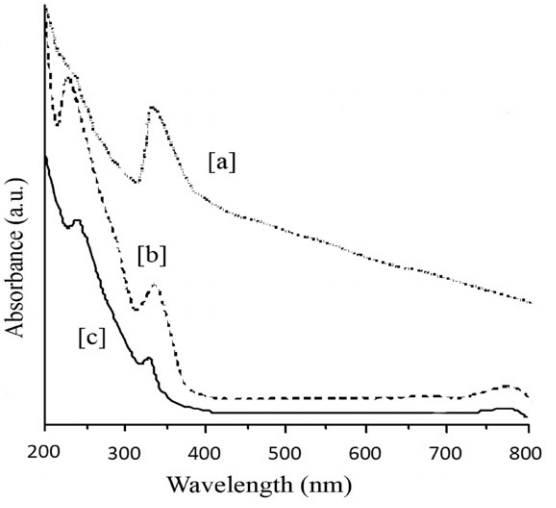

Figure 4. The electronic spectra of (a) VTCH Schiff base, (b) Neat $Co(VTCH)_2$, and (c) $[Co(VTCH)_2]$-Y.

Table 5. Oxidation of cyclohexane to cyclohexanol and cyclohexanone with 30% H_2O_2 catalyzed by ZENMs.

Sr. no.	Compounds	Conversion (%)	Selectivity (%)	
			CyOL	CyONE
1	$[Mn(VTCH)_2]$-Y	12.4	29.3	70.7
2	$[Mn(VFCH)_2]$-Y	10.9	25.6	74.4
3	$[Co(VTCH)_2]$-Y	23.6	27.1	72.9
4	$[Co(VFCH)_2]$-Y	21.8	34.7	65.3
5	$[Ni(VTCH)_2]$-Y	16.9	45.2	54.8
6	$[Ni(VFCH)_2]$-Y	15.4	40.6	59.4
7	$[Cu(VTCH)_2]$-Y	36.7	18.1	81.9
8	$[Cu(VFCH)_2]$-Y	35.1	24.2	75.8
9	$[Cu(VTCH)_2]$-Y[a]	34.8	20.3	79.7
10	$[Cu(VTCH)_2]$-Y[b]	32.6	21.7	78.3

CyOL is cyclohexane-1-ol product; CyONE is cyclohexane-1-one product.
[a]First reused catalyst.
[b]Second reused catalyst.

catalytically active. Figure 5 summarizes the percentage conversion of cyclohexane along with cyclohexanol and cyclohexanone formations. Selectivity of cyclohexanone formation varied (54.8–81.9%) from catalyst to catalyst; all these catalysts are selective toward the cyclohexanone formation.

The coordinatively unsaturated M(II) (where M = Mn(II), Co(II), Ni(II), and Cu(II)) species within nanocages of zeolite-Y play a crucial role in enhancing catalytic performance. Scheme 1 demonstrates a possible mechanism for catalytic oxidation of cyclohexane. The first step involves formation of metal-peroxo species, which have powerful oxidation ability [54, 55]. In the next step, formation of intermediate species

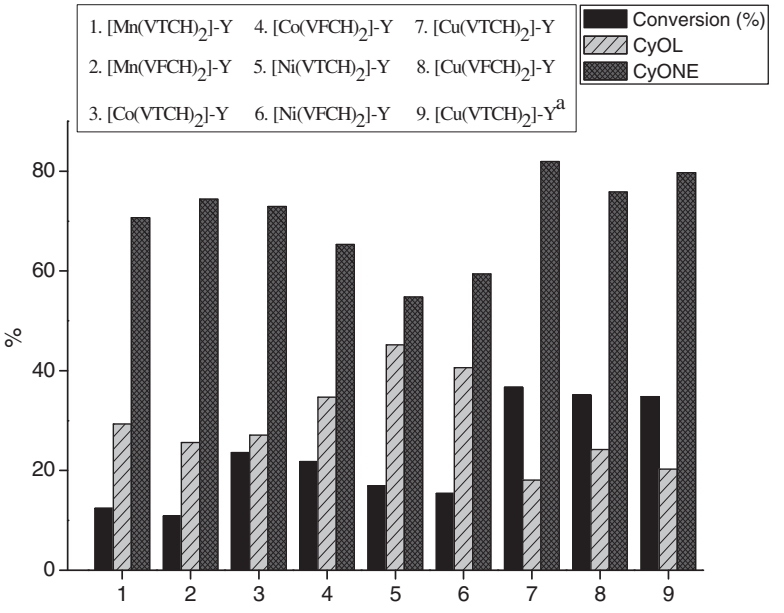

Figure 5. Conversion % of oxidation of cyclohexane.
[a]First reused catalyst.

transfers the coordinated oxygen to the substrate to obtain product. In the case of $[M(VTCH)_2]$-Y or $[M(VFCH)_2]$-Y (where M = Ni, Co, or Mn) slow formation of peroxo species with H_2O_2 or sluggishness to transfer of peroxo oxygen to the substrate limits the reaction. In contrast, the performance of $[Cu(VTCH)_2]$-Y is much better, giving highest percentage conversion of CyONE (table 5). To achieve suitable reaction conditions for maximum oxidation, parameters such as effect of amount of catalyst and effect of temperature were studied using $[Cu(VTCH)_2]$-Y as a representative catalyst. The results of these effects along with their possible explanations are summarized below.

3.3.2. Effect of amount of catalysts. The amount of catalyst has a significant effect on the oxidation of cyclohexane. Four different amounts of $[Cu(VTCH)_2]$-Y catalyst namely 40, 50, 60, and 65 mg were used, keeping all other reaction parameters unchanged (temperature (80°C), cyclohexane (10 mmol), 30% H_2O_2 (10 mmol) in acetonitrile (2 mL), and reaction time (2 h)). The results are shown in figure 6, indicating 28.5%, 35.7%, 36.7%, and 36.7% conversion corresponding to 40, 50, 60, and 65 mg catalyst, respectively. Lower conversion of cyclohexane with 40 and 50 mg catalyst may be due to fewer catalytic sites. The greater conversion percentage was observed with 60 mg catalyst but there was no difference in the progress of reaction when more than 65 mg of catalyst was employed. Therefore, 60 mg amount of catalyst was taken to be optimal.

3.3.3. Effect of temperature. For four different temperatures namely 60°C, 70°C, 75°C, and 80°C, the oxidation of cyclohexane (figure 7) was examined under the

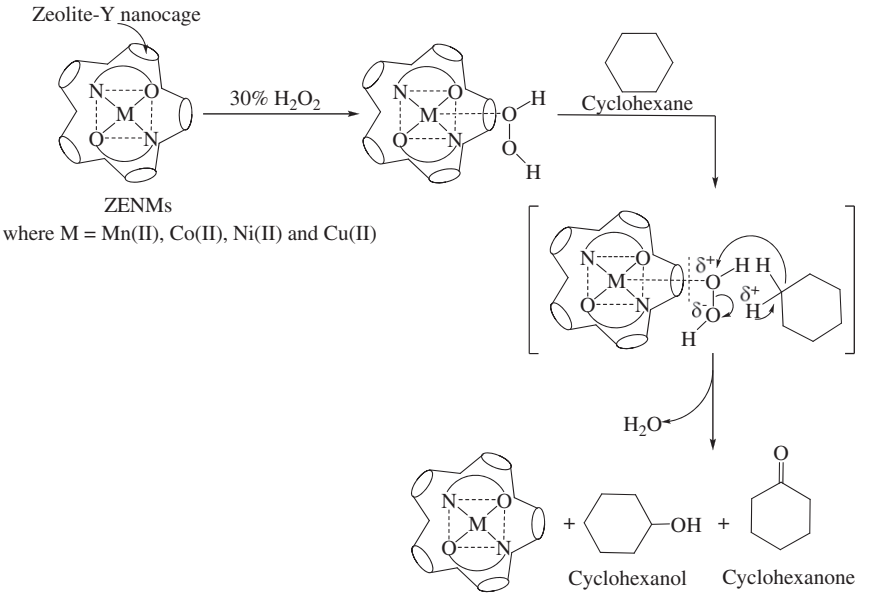

Scheme 1. The proposed mechanism illustrating the formation of cyclohexanol and cyclohexanone in catalytic oxidation of cyclohexane.

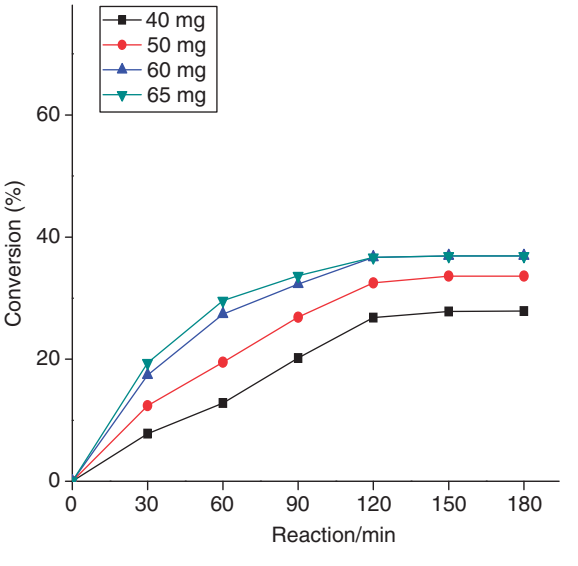

Figure 6. Effect of amount of catalyst on the oxidation of cyclohexane.

above reaction conditions, cyclohexane (10 mmol), 30% H_2O_2 (10 mmol), catalyst (60 mg) in acetonitrile (2 mL) for 2 h. On increasing the temperature from 60°C to 80°C, improvements were observed with no change in percentage conversion for oxidation of cyclohexane, consequently at 80°C for 2 h time is considered to be the optimum.

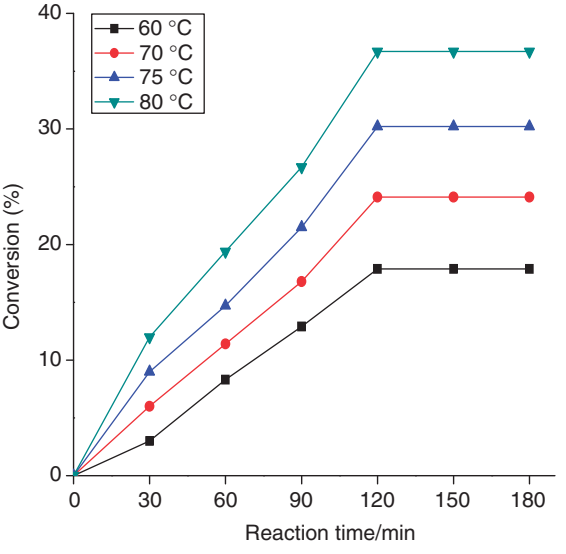

Figure 7. Effect of temperature on the oxidation of cyclohexane.

3.3.4. Test for recyclability. $[Cu(VTCH)_2]$-Y was recycled for oxidation of cyclohexane to establish the effect of encapsulation on stability. The initial run shows a conversion of 35.1% and it was just marginally reduced to 34.8% and 32.6% after first and second recycling of the catalyst, respectively. These results indicate that $[Cu(VTCH)_2]$-Y can be recycled for oxidation of cyclohexane without much loss in activity. Consequently, the encapsulation of metal complexes inside the nanocavity of zeolite-Y increases the life of catalyst by reducing dimerization due to restriction of internal framework structure.

4. Conclusions

The results obtained in this study allow the following conclusions:

(1) Manganese(II), cobalt(II), nickel(II), and copper(II) complexes of VTCH and/or VFCH have been encapsulated in the nanocages of zeolite-Y, leading to the formation of ZENMs. Chemical analysis, spectroscopic studies, BET, SEMs, and XRD patterns present clear evidence for encapsulation.
(2) Among these nanohybrid materials, $[Cu(VTCH)_2]$-Y catalyzes the oxidation of cyclohexane with very good yield of cyclohexanone selectively, which is followed by $[Cu(VFCH)_2]$-Y which in turn is better than $[Mn(VFCH)_2]$-Y and so on.
(3) Under the best reaction conditions, the selectivity of cyclohexanone formation is about 81.9% with $[Cu(VTCH)_2]$-Y catalyst.
(4) The test for recyclability using $[Cu(VTCH)_2]$-Y as a representative catalyst has been carried out. The results reflect the reusability of the nanohybrid materials as not much loss in their catalytic activity was noticed.

Acknowledgments

We express our gratitude to the Head, Department of Chemistry, Bhavnagar University, Bhavnagar, India for providing the necessary laboratory facilities. Mr Parthiv M. Trivedi would like to acknowledge UGC, Delhi for providing meritorious fellowship. An analytical facility provided by the CSMCRI and Department of Physics, Bhavnagar University, Bhavnagar, India is gratefully acknowledged.

References

[1] K.U. Ingold. *Aldrichim. Acta*, **22**, 69 (1989).
[2] U. Schuchardt, W.A. Carvalho, E.V. Spinacé. *Synlett*., **10**, 713 (1993).
[3] M.C. Esmelindro, E.G. Oestreicher, H.M. Alvarez, C. Dariva, S.M. Egues, C. Fernandes, A.J. Bortoluzzi, V. Drago, O.A.C. Antunes. *J. Inorg. Biochem*., **99**, 2054 (2005).
[4] M.H.N. Olsen, G.C. Salomaõ, C. Fernandes, V. Drago, A. Horn, L.C. Filho, O.A.C. Antunes. *J. Supercrit. Fluids*, **34**, 119 (2005).
[5] H.A. Wittcoff, B.G. Reuben. *Industrial Organic Chemicals*, Wiley & Sons, New York (1996).
[6] U. Schuchardt, R. Pereira, M. Rufo. *J. Mol. Catal. A: Chem*., **135**, 257 (1998).
[7] U. Schuchardt, D. Cardoso, R. Sercheli, R. Pereira, R.S. Da Cruz, M.C. Guerreiro, D. Mandelli, E.V. Spinacé, E.L. Pires. *Appl. Catal. A: Gen*., **211**, 1 (2001).
[8] A. Corma, H. Garcia. *Chem. Rev*., **102**, 3837 (2002).
[9] T. Sato, J. Dakka, R.A. Sheldon. *J. Chem. Soc., Chem. Commun*., 1887 (1994).
[10] M.A. Camblor, A. Corma, A. Martinez, J.P. Parienta. *J. Chem. Soc., Chem. Commun*., 589 (1992).
[11] G. Tozzola, M.A. Mantegazza, G. Ranghino, G. Petrini, S. Bordiga, G. Ricchiardi, C. Lamberti, R. Zulian, A. Zecchina. *J. Catal*., **179**, 64 (1998).
[12] A.P. Singh, T. Selvam. *J. Mol. Catal. A: Chem*., **113**, 489 (1996).
[13] B.F. Sels, D. De Vos, P.A. Jacobs. *Tetrahedron Lett*., **37**, 8557 (1996).
[14] T. Joseph, D. Srinivas, C.S. Gopinath, S.B. Halligudi. *Catal. Lett*., **83**, 209 (2002).
[15] T. Joseph, S.B. Halligudi. *J. Mol. Catal. A: Chem*., **229**, 241 (2005).
[16] R.A. Sheldon, I.W.C.E. Arends, A. Dijksman. *Catal. Today*, **57**, 157 (2000).
[17] C.R. Jacob, S.P. Verkey, P. Ratnasamy. *Microporous Mesoporous Mater*., **22**, 465 (1998).
[18] G.J. Hutchings. *Chem. Commun*., 301 (1999).
[19] M.J. Alcón, A. Corma, M. Iglesias, F. Sánchez. *J. Mol. Catal. A: Chem*., **178**, 253 (2002).
[20] M.R. Maurya, A. Kumar, J.C. Pessoa. *J. Coord. Chem. Rev*., **255**, 2315 (2011).
[21] P. Parpot, C. Teixeir, A.M. Almeid, C. Ribeiro, I.C. Neves, A.M. Fonseca. *Microporous Mesoporous Mater*., **117**, 297 (2009).
[22] S.R. Batten, R. Robson. *Angew. Chem. Int. Ed*., **37**, 1460 (1998).
[23] N.W. Ockwig, O.D. Friedrichs, M. O'Keeffe, O.M. Yaghi. *Acc. Chem. Res*., **38**, 176 (2005).
[24] S. Kitagawa, R. Kitaura, S. Noro. *Angew. Chem. Int. Ed*., **43**, 2334 (2004).
[25] J.L.C. Rowsell, E.C. Spencer, J. Eckert, J.A.K. Howard, O.M. Yaghi. *Science*, **309**, 1350 (2005).
[26] O.M. Yaghi, G. Li, H. Li. *Nature*, **378**, 703 (1995).
[27] M. Fujita, Y.J. Kwon, S. Washizu, K. Ogura. *J. Am. Chem. Soc*., **116**, 1151 (1994).
[28] J.S. Seo, D. Whang, H. Lee, S.I. Jun, J. Oh, Y.J. Jeon, K. Kim. *Nature*, **404**, 982 (2000).
[29] L.-G. Qiu, A.-J. Xie, L.-D. Zhang. *Adv. Mater*., **17**, 689 (2005).
[30] T. Sawaki, T. Dewa, Y. Aoyama. *J. Am. Chem. Soc*., **120**, 8539 (1998).
[31] C.-D. Wu, W. Lin. *Angew. Chem. Int. Ed*., **46**, 1075 (2007).
[32] R.Q. Zou, H. Sakurai, Q. Xu. *Angew. Chem. Int. Ed*., **45**, 2542 (2006).
[33] D.N. Dybtsev, A.L. Nuzhdin, H. Chun, K.P. Bryliakov, E.P. Talsi, V.P. Fedin, K. Kim. *Angew. Chem. Int. Ed*., **45**, 916 (2006).
[34] L. Alaerts, E. Seguin, H. Poelman, F. Thibault-Starzyk, P.A. Jacobs, D.E. De Vos. *Chem. Eur. J*., **12**, 7353 (2006).
[35] C.D. Wu, A. Hu, L. Zhang, W.B. Lin. *J. Am. Chem. Soc*., **127**, 8940 (2005).
[36] F.X.L.I. Xamena, A. Abad, A. Corma, H. Garcia. *J. Catal*., **250**, 294 (2007).
[37] K.L. Wong, G.L. Law, Y.-Y. Yang, W.T. Wong. *Adv. Mater*., **18**, 1051 (2006).
[38] M. Alvaro, E. Carbonell, B. Ferrer, F.X.L.I. Xamena, H. Garcia. *Chem. Eur. J*., **13**, 5106 (2007).
[39] F.X.L.I. Xamena, A. Corma, H. Garcia. *J. Phys. Chem. C*, **111**, 80 (2007).
[40] G.J. Halder, C.J. Kepert, B. Moubaraki, K.S. Murray, J.D. Cashion. *Science*, **298**, 1762 (2002).
[41] M. Heitbaum, F. Glorious, I. Escher. *Angew. Chem. Int. Ed*., **45**, 4732 (2006).

[42] K.O. Xavier, J. Chacko, K.K. Mohammed Yusuff. *Appl. Catal. A: Gen.*, **258**, 251 (2004).
[43] B. Dutta, S. Jana, R. Bera, P.K. Saha, S. Koner. *Appl. Catal. A: Gen.*, **318**, 89 (2007).
[44] P. Chen, B. Fan, M. Song, C. Jin, J. Ma, R. Li. *Catal. Commun.*, **7**, 969 (2006).
[45] C.K. Modi, D.H. Jani, H.S. Patel, H.M. Pandya. *Spectrochim. Acta, Part A*, **75**, 1321 (2010).
[46] M. Salavati-Niasari, M. Shakouri-Arani, F. Davar. *Microporous Mesoporous Mater.*, **116**, 77 (2008).
[47] C.K. Modi, D.H. Jani. *Appl. Organomet. Chem.*, **25**, 429 (2011).
[48] C.K. Modi, D.H. Jani. *J. Therm. Anal. Calorim.*, **102**, 1001 (2010).
[49] A.H. Ahmed, A.G. Mostafa. *Mater. Sci. Eng. C*, **29**, 877 (2009).
[50] K. Mukkanti, K.B. Pandeya, R.P. Singh. *Synth. React. Inorg. Met.-Org. Chem.*, **16**, 229 (1986).
[51] A.B.P. Lever. *Inorganic Electronic Spectroscopy*, 2nd Edn, p. 411, Elsevier, Amsterdam (1984).
[52] S.A. Sallam. *J. Coord. Chem.*, **60**, 951 (2007).
[53] M. Ghadiri, M. Farzaneh, M. Ghandi, M. Alizadeh. *J. Mol. Catal. A: Chem.*, **233**, 127 (2005).
[54] L. Jian, C. Chen, F. Lan, S. Deng, W. Xiao, N. Zhang. *Solid State Sci.*, **13**, 1127 (2011).
[55] B. Xiao, H.W. Hou, Y.T. Fan. *J. Organomet. Chem.*, **692**, 2014 (2007).